ЖЭТФ, 2014, том 146, вып. 3 (9), стр. 448–454

K-SHELL X-RAY INTENSITY RATIOS AND VACANCY TRANSFER PROBABILITIES OF Pt, Au, AND Pb BY A SIMPLE METHOD

L. F. M. Anand [a], ***S. B. Gudennavar*** [a*], ***S. G. Bubbly*** [a], ***B. R. Kerur*** [b]

[a] *Department of Physics, Christ University*
Bangalore-560029, Karnataka, India

[b] *Department of Physics, Gulbarga University*
Gulbarga-585106, Karnataka, India

Received January 8, 2014

The K-shell X-ray intensity ratios, radiative and total vacancy transfer probablities of platinum, gold, and lead are measured by employing the 2π-geometrical configuration and a weak gamma source, a simple method proposed previously by our group. The targets of Pt, Au, and Pb were excited using γ-rays of weighted energy 123.6 keV from a weak ^{57}Co source and the emitted K-shell X-rays were detected using an HPGe X-ray detector spectrometer coupled to a 16k multichannel analyzer. The measured values of these parameters are compared with the theoretical values and experimental data of other researchers, finding a good agreement. Thus 2π-geometrical configuration method with a weak gamma source can be alternative simple method to measure various atomic parameters in the field of X-ray spectroscopy.

DOI: 10.7868/S0044451014090041

1. INTRODUCTION

The accurate values of K-shell X-ray intensity ratios, radiative and total vacancy transfer probablities of elements are essential in the fields of atomic, molecular, and nuclear physics, and material science [1–5]. These X-ray fluorescence parameters are also important in studies of the electron capture process, internal conversion electron process, photoelectric effect, and radiative and nonradiative probabilities [6–10]. Over the years, several researchers have measured K-shell X-ray intensity ratios and vacancy transfer probabilities using various methods and detectors [11–14]. However, these methods involve complicated single and double reflection geometries, which require strong gamma sources of the order of 10^9 Bq or more. In this paper, we measure these parameters for platinum, gold, and lead using a simple method proposed previously by our group [15–19], which adopts a 2π-geometrical configuration and weak gamma sources.

*E-mail: shivappa.b.gudennavar@christuniversity.in

2. THEORY

The total vacancy transfer probability from the K shell to L_i shells of an atom is the sum of radiative vacancy transfer probability $\eta_{KL_i}(R)$ and the nonradiative vacancy transfer probability $\eta_{KL_i}(A)$:

$$\eta_{KL} = \eta_{KL_i}(R) + \eta_{KL_i}(A). \tag{1}$$

The K–L_i radiative vacancy transfer probability is given by

$$\eta_{KL_i}(R) = \omega_K \frac{I(KL_i)}{I_K(R)}, \tag{2}$$

where $I(KL_i)$ is the K–L_i X-ray intensity, $I_K(R)$ is the total intensity of K-shell X-rays, and ω_K is the K-shell X-ray fluorescence yield. Because the K-to-L_1 radiative transition is forbidden, we have only K–L_2 and K–L_3 transitions and the corresponding radiative vacancy transfer probabilities [1] are given by

$$\eta_{KL_2}(R) = \omega_K \frac{I(K_{\alpha_2})}{I(K_{\alpha_1})} \times$$
$$\times \left\{ \left[1+\frac{I(K_{\alpha_2})}{I(K_{\alpha_1})}\right] \left[1+\frac{I(K_\beta)}{I(K_\alpha)}\right] \right\}^{-1} = \omega_K \frac{I(K_{\alpha_2})}{I_K(R)}, \tag{3}$$

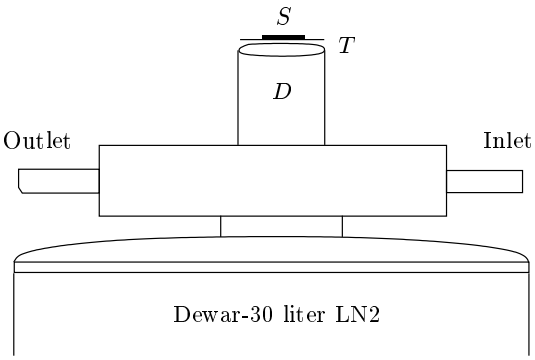

Fig. 1. Experimental arrangement: S — source; T — target; D — HPGe detector

$$\eta_{K\,L_3}(R) = \omega_K \left\{ \left[1 + \frac{I(K_{\alpha_2})}{I(K_{\alpha_1})} \right] \left[1 + \frac{I(K_\beta)}{I(K_\alpha)} \right] \right\}^{-1} = \omega_K \frac{I(K_{\alpha_1})}{I_K(R)}. \quad (4)$$

The probability for the radiative transfer of a vacancy from the K to M shell of an atom is given by

$$\eta_{K\,M}(R) = \omega_K \frac{I(K_{\beta_1'})}{I(K_{\alpha_1})} \times \left\{ \left[1 + \frac{I(K_{\alpha_2})}{I(K_{\alpha_1})} \right] \left[1 + \frac{I(K_\beta)}{I(K_\alpha)} \right] \right\}^{-1} = \omega_K \frac{I(K_{\beta_1'})}{I_K(R)}, \quad (5)$$

where $I(K_{\beta_1'}) = I(K_{\beta_1}) + I(K_{\beta_3})$.

The total vacancy transfer probability from the K shell to the L shell can be expressed in terms of the K-shell X-ray fluorescence yield ω_K and the K-shell X-ray intensity ratio $I(K_\beta)/I(K_\alpha)$ [20] as

$$\eta_{KL} = \frac{2 - \omega_K}{1 + I(K_\beta)/I(K_\alpha)}. \quad (6)$$

The intensity ratio of characteristic X-rays of type i to type j is given by

$$\frac{I(i)}{I(j)} = \frac{I'(i)\varepsilon_j \beta_j \exp(-\mu_{xjw} t_w)}{I'(j)\varepsilon_i \beta_i \exp(-\mu_{xiw} t_w)}, \quad (7)$$

where $I'(i)$ and $I'(j)$ are the measured intensities of K-shell X-rays of types i and j; $i = K_{\alpha_2}, K_{\beta_1'}, K_\beta$, $j = K_{\alpha_1}, K_{\alpha_1}, K_\alpha$; ε_i and ε_j are efficiencies of the detector for K-shell X-rays of types i and j; β_i and β_j are the self-attenuation correction factors for K-shell X-rays of types i and j in the target material and are calculated using Eq. (8); $\exp(-\mu_{xiw} t_w)$ and $\exp(-\mu_{xjw} t_w)$ are the detector window attenuation correction factors for K-shell X-rays of types i and j; here μ_{xiw} and μ_{xjw} are the mass attenuation coefficients [cm^2/gm] of K-shell X-rays of types i and j in the detector window of thickness t_w [g/cm^2].

Taking the isotropic emission of K-shell X-rays into account and recalling that we measure the intensity of all K-shell X-rays emerging from the target in all forward directions, that is, emitting into a solid angle of nearly 2π sr, we use the correction factor β without involving the scattering angles:

$$\beta = \frac{1 - \exp\left[-(\mu_i + \mu_e)t\right]}{(\mu_i + \mu_e)t}, \quad (8)$$

where t is the target thickness [g/cm^2], and μ_i and μ_e are the respective mass attenuation coefficients [cm^2/gm] of incident and emitted K-shell X-rays in the target. These coefficients have been computed using WinXcom software [21]. Following the target thickness criterion in Ref. [2], we have found that the targets of the thickness with β values in the range $0.75 \le \beta \le 0.95$ are suitable for accurate determination of K-shell X-ray fluorescence parameters (for details, see Refs. [15–19]).

3. EXPERIMENTAL

The schematic diagram of the experimental arrangement is shown in Fig. 1. In the present investigation, we used an X-ray detector spectrometer consisting of a HPGe detector (active area 500 mm^2, 10 mm thick high-purity n-type germanium crystal, Be window 0.6 mm in thickness) coupled to a 16k multichannel analyzer (DSA-1000). The energy resolution of the HPGe detector (Model: GL0510P, procured from Canberra USA) is 200 eV at 5.9 keV. The dead layer of the detector is 0.7 mm. The distance from the cryostat window (Be) to the detector material is 5 mm. The HPGe detector is operational in the energy range 3 to 500 keV. This detector is cooled to 77 K using a liquid-nitrogen cryostat. The coolant liquid nitrogen is filled in the cryostat through the inlet and the air escapes from the outlet (Fig. 1). The spectrometer is calibrated and standardized using various gamma and X-ray sources.

A ^{57}Co radioactive source with a strength of the order of 10^4 Bq is used as the excitation source. We used the photon energy 123.6 keV, i. e., the weighted average of 122 and 136 keV, in the calculation of mass attenuation coefficients μ_i, which are required in the calculation of the self-attenuation correction factor β. The target materials were pure elements (99.99 %). Platinum was procured in the form of thin foil of the required thickness from Alfa Aesar A Johnson Matthey Company UK, whereas high-purity gold and lead targets were purchased from a local company.

Table 1. The measured values of K-shell X-ray intensity ratios for Pt, Au, and Pb along with the theoretical and others' experimental values

Element	Parameter	Present	Theoretical values [23]	Others' experimental	References
Platinum ($Z = 78$)	$\frac{I(K_{\alpha_2})}{I(K_{\alpha_1})}$	0.597 ± 0.010	0.585	0.584	[11]
				0.574 ± 0.026	[24]
				0.583	[1]
				0.563	[28]
	$\frac{I(K_{\beta_1'})}{I(K_{\alpha_1})}$	0.340 ± 0.010	0.328	0.322	[11]
				0.328 ± 0.026	[24]
	$\frac{I(K_{\beta_2})}{I(K_{\alpha_1})}$	0.108 ± 0.011	0.089	0.0896	[11]
				0.084	[24]
	$\frac{I(K_{\beta})}{I(K_{\alpha})}$	0.260 ± 0.006	0.263	0.259	[11]
				0.2682 ± 0.005	[29]
				0.275	[1]
Gold ($Z = 79$)	$\frac{I(K_{\alpha_2})}{I(K_{\alpha_1})}$	0.583 ± 0.011	0.588	0.618	[12]
				0.591 ± 0.032	[24]
				0.585 ± 0.004	[25]
				0.584 ± 0.012	[30]
				0.57 ± 0.03	[31]
	$\frac{I(K_{\beta_1'})}{I(K_{\alpha_1})}$	0.336 ± 0.011	0.329	0.585	[28]
				0.357	[12]
				0.333 ± 0.021	[24]
				0.329 ± 0.003	[25]
				0.333 ± 0.011	[30]
				0.210 ± 0.02	[31]
	$\frac{I(K_{\beta_2})}{I(K_{\alpha_1})}$	0.089 ± 0.015	0.091	0.091 ± 0.004	[24]
				0.098 ± 0.005	[30]
				0.11 ± 0.01	[31]
	$\frac{I(K_{\beta})}{I(K_{\alpha})}$	0.264 ± 0.010	0.265	0.280	[12]
				0.2680 ± 0.005	[29]
				0.262 ± 0.003	[25]
				0.210 ± 0.012	[30]
				0.210 ± 0.03	[31]

The intensities of K-shell X-rays were measured as follows. The "source with background spectrum" was acquired first, by placing the source on the face of the detector for the live time of 2000 s to minimize the uncertainties in the results due to counting statistics. The "transmitted spectrum with background" was then acquired by sandwiching the target between the source and the detector window. By subtracting the former from the latter, we obtain a clean fluorescence K-shell X-ray spectrum that corresponds to the target element

Table 1

Element	Parameter	Present	Theoretical values [23]	Others' experimental	References
Lead ($Z = 82$)	$\frac{I(K_{\alpha_2})}{I(K_{\alpha_1})}$	0.596 ± 0.010	0.595	0.606 ± 0.042	[24]
				0.594 ± 0.003	[25]
				0.593 ± 0.019	[26]
				0.592	[1]
				0.589 ± 0.012	[30]
				0.590 ± 0.03	[31]
				0.596	[28]
	$\frac{I(K_{\beta_1'})}{I(K_{\alpha_1})}$	0.330 ± 0.008	0.334	0.296 ± 0.019	[24]
				0.332 ± 0.002	[25]
				0.343 ± 0.026	[26]
				0.333 ± 0.011	[30]
	$\frac{I(K_{\beta_2})}{I(K_{\alpha_1})}$	0.085 ± 0.01	0.096	0.087 ± 0.004	[24]
				0.098 ± 0.005	[30]
				0.11 ± 0.01	[31]
	$\frac{I(K_{\beta})}{I(K_{\alpha})}$	0.262 ± 0.006	0.270	0.279	[1]
				0.268 ± 0.003	[25]
				0.275 ± 0.019	[26]
				0.2822 ± 0.007	[29]
				0.271 ± 0.011	[30]
				0.207 ± 0.018	[31]

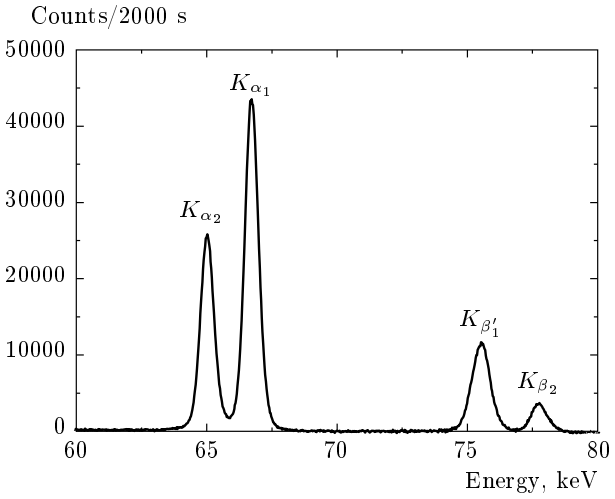

Fig. 2. K-shell X-ray fluorescence spectrum of platinum

under investigation (Fig. 2). Each K-shell X-ray peak is fitted to a Gaussian distribution function using the ORIGIN software for estimating the area under the peak. The area under each peak gives the intensity of the K-shell X-ray of a given type, which is then corrected for self-attenuation in the target, attenuation in the window of the detector, efficiently of the detector, and the dead layer attenuation to obtain the total number of K-shell X-rays emitted into the forward hemisphere. The K-shell X-ray intensity ratios and the radiative and the total vacancy transfer probabilities were calculated using Eqs. (7) and (3)–(6). The vacancy transfer probabilities of the elements were calculated using the K-shell X-ray fluorescence yield (ω_K) values from Hubbell tables [3], Krause [22], and Bambynek et al. [2]. The experiment was repeated four times for each element and the weighted average of the four trials has been presented.

Table 2. The present experimental values of radiative and total vacancy transfer probabilities for Pt, Au, and Pb along with the theoretical and others' experimental values

Parameter	Using ω_K from Hubbell [3]	Using ω_K from Bambynek et al. [2]	Using ω_K from Krause [22]	Theory	Others' experimental
Platinum ($Z = 78$)					
$\eta_{KL_2}(R)$	0.282 ± 0.002	0.284 ± 0.014	0.283 ± 0.014	0.278 [10]	$-^*$
$\eta_{KL_3}(R)$	0.473 ± 0.003	0.477 ± 0.035	0.475 ± 0.035	0.477 [10]	$-^*$
$\eta_{KM}(R)$	0.160 ± 0.001	0.161 ± 0.011	0.161 ± 0.011	$-^*$	$-^*$
η_{KL}	0.826 ± 0.009	0.820 ± 0.009	0.823 ± 0.009	0.819 [11]	0.808 [14]
				0.819 [32]	0.883 [11]
				0.813 [1]	0.817 [32]
Gold ($Z = 79$)					
$\eta_{KL_2}(R)$	0.285 ± 0.005	0.286 ± 0.019	0.286 ± 0.019	0.292 [23]	0.280 ± 0.005 [25]
$\eta_{KL_3}(R)$	0.480 ± 0.004	0.482 ± 0.012	0.482 ± 0.012	0.492 [23]	0.479 ± 0.008 [25]
$\eta_{KM}(R)$	0.162 ± 0.004	0.163 ± 0.023	0.163 ± 0.023	$-^*$	$-^*$
η_{KL}	0.822 ± 0.010	0.818 ± 0.011	0.818 ± 0.011	0.811 [1]	0.812 [12]
				0.816 [23]	0.821 ± 0.004 [33]
				0.817 [20]	0.820 ± 0.024 [32]
				0.815 [32]	0.815 ± 0.008 [27]
Lead ($Z = 82$)					
$\eta_{KL_2}(R)$	0.289 ± 0.002	0.292 ± 0.020	0.290 ± 0.020	0.293 [34]	0.283 ± 0.004 [25]
				0.293 [23]	0.281 ± 0.022 [26]
				0.281 [1]	
$\eta_{KL_3}(R)$	0.483 ± 0.003	0.487 ± 0.009	0.485 ± 0.009	0.475 [34]	0.477 ± 0.006 [25]
				0.493 [23]	0.474 ± 0.038 [26]
				0.475 [1]	
$\eta_{KM}(R)$	0.171 ± 0.001	0.173 ± 0.013	0.172 ± 0.013	0.165 [23]	0.163 ± 0.009 [26]
η_{KL}	0.821 ± 0.010	0.803 ± 0.008	0.807 ± 0.008	0.806 [1]	0.814 ± 0.006 [33]
				0.809 [23]	0.809 ± 0.040 [32]
				0.806 [34]	0.805 ± 0.012 [27]
				0.811 [20]	
				0.810 [32]	

*Values not available.

4. RESULTS AND DISCUSSION

The K-shell X-ray intensities for Pt, Au, and Pb have been measured adopting the procedure explained in the preceding section. The K-shell X-ray intensity ratios for these elements along with the theoretical values of Scofield [23] and others' experimental values obtained by adopting reflection geometries are compared in Table 1. From Table 1, we see that our results agree fairly well with the theoretical and others' experimental values of K-shell X-ray intensity ratios of the elements investigated. The measured K-shell X-ray intensity ratios for these elements have a 2 to 3.8 % uncertainty, which comes from counting statistics (less

than 3 %), the target thickness and self-attenuation correction factor (1 %), window attenuation correction (less than 1 %), and the detection efficiency of the detector (less than 1 %). The $I(K_{\alpha_2})/I(K_{\alpha_1})$ intensity ratio for platinum differs by 1–2 % with reference to Scofield [23], Cengiz et al. [11], and Apaydin et al. [24], by 0.5–3.5 % with reference to Scofield [23], Cengiz et al. [12], Apaydin et al. [24], and Bennal et al. [25] for gold, and by 0.1–1 % with reference to Scofield [23], Bennal et al. [25], Durak and Ozdemir [26], and Apaydin et al. [24] for lead. The $I(K_{\beta_1'})/I(K_{\alpha_1})$ intensity ratio differs by 1–2 % with reference to the theoretical value of Scofield [23] for platinum, by 0.7–2 % with reference to Scofield [23], Cengiz et al. [12], and Bennal et al. [25] for gold, and by 0.2–1.3 % with reference to Scofield [23], Bennal et al. [25], and Durak and Ozdemir [26] for lead. The percentage difference between the present work and the references cited in Table 1 is as small as 0.2 to 1.9 % for the ratio $I(K_{\beta_2})/I(K_{\alpha_1})$. Similarly, there is a difference of 0.1–1.6 % between our measured $I(K_\beta)/I(K_\alpha)$ intensity ratios and the values from the references cited in Table 1 for all the target elements.

The radiative and total vacancy transfer probabilities for these elements have been determined using the experimentally measured K-shell X-ray intensity ratios and the ω_K values taken from Hubbell tables [3], Krause [22], and Bambynek et al. [2]. These results are presented in Table 3 along with the theoretical and others' experimental values for comparison. It is found that the radiative vacancy transfer probabilities determined using the ω_K values from Hubbell tables [3] for platinum differ by 1.3–1.8 % with reference to Cengiz et al. [11], Apaydin et al. [24], Ertuğral et al. [27], and the theoretical estimation of Cengiz et al. [11], by 0.1–1.1 % with reference to Scofield [23], Schönfield and Janßen [20], Bennal et al. [25], Ertuğral et al. [27], Cengiz et al. [12], and Rao et al. [1] for gold, and by about 1.6 % for lead with reference to all the references cited in Table 2. We note that the radiative vacancy transfer probabilities deremnined using the ω_K values from Krause [22] and Bambynek et al. [2] differ by 0.1 to 2 % from the radiative vacancy transfer probabilities determined using the ω_K values from Hubbell tables [3]. The calculated total vacancy transfer probability values in the present work using the K-shell X-ray fluorescence yield values from Hubbell tables [3] carry an uncertainty of 1–2 % for all the elements. This uncertainty is again less than 2 % when ω_K values for the calculation of η_{KL} are taken from Bambynek et al. [2] and it decreases to 0.2 % when ω_K values from Krause [22] are used.

The present study shows that the simple 2π-geometrical configuration method with an HPGe detector and a weak radioactive source can be an alternative simple method for the measurement of K-shell X-ray intensity ratios and the K–L_i and K–M radiative and total vacancy transfer probabilities of elements. To the best of our knowledge, the radiative vacancy transfer probabilities ($\eta_{KL_2}(R)$, $\eta_{KL_3}(R)$, and $\eta_{KM}(R)$) for platinum are reported for the first time.

The authors acknowledge the help received from A. Manjunath, Department of Physics, Gulbarga University, and M. T. Rameshan, Christ University, in conducting the experiments.

REFERENCES

1. P. V. Rao, M. H. Chen, and B. Crasemann, Phys. Rev. A **5**, 997 (1972).
2. W. Bambynek, B. Crasemann, R. W. Fink et al., Rev. Mod. Phys. **44**, 716 (1972).
3. J. H. Hubbell, NISTIR, 89 (1989).
4. G. R. Lachance and F. Claisse, *Quantitative X-ray Fluorescence Analysis*: *Theory and Application*, Wiley, New York (1995).
5. U. Bergmann, P. Glatzel, F. deGroot, and S. P. Cramer, J. Amer. Chem. Soc. **121**, 4926 (1999).
6. J. P. Hurley and J. M. Ferguson, Nucl. Phys. **27**, 75 (1961).
7. H. Primakoff and F. T. Porter, Phys. Rev. **89**, 930 (1953).
8. T. Mukoyama, K. Taniguchi, and H. Adachi, Adv. Quantum. Chem. **37**, 139 (2000).
9. E. Arndt, G. Brunner, and E. Hartmann, J. Phys. B **15**, 887 (1982).
10. N. V. Rao, S. B. Reddy, and D. L. Sastry, Nuovo Cim. **97**, 1 (1987).
11. E. Cengiz, E. Tıraşoğlu, G. Apaydin et al., Radiat. Phys. Chem. **80**, 328 (2011).
12. E. Cengiz, E. Tıraşoğlu, V. Aylikci, and G. Apaydin, Radiat. Phys. Chem. **79**, 809 (2010).
13. T. L. Hopman, C. M. Heirwegh, J. L. Campbell et al., X-ray Spectrom. **41**, 164 (2012).
14. G. Apaydin and E. Tıraşoğlu, Radiat. Phys. Chem. **81**, 1593 (2012).

15. L. D. Horakeri, B. Hanumaiah, and S. R. Thontadarya, X-ray Spectrom. **26**, 69 (1997).

16. L. D. Horakeri, B. Hanumaiah, and S. R. Thontadarya, X-ray Spectrom. **27**, 344 (1998).

17. S. B. Gudennavar, N. M. Badiger, S. R. Thontadarya, and B. Hanumaiah, Radiat. Phys. Chem. **68**, 721 (2003).

18. S. B. Gudennavar, N. M. Badiger, S. R. Thontadarya, and B. Hanumaiah, Radiat. Phys. Chem. **68**, 745 (2003).

19. L. D. Horakeri, S. G. Bubbly, and S. B. Gudennavar, Radiat. Phys. Chem. **80**, 626 (2011).

20. E. Schönfield and H. Janßen, Nucl. Instr. Meth. A **369**, 527 (1996).

21. M. J. Berger, J. H. Hubbell, S. M. Seltzer et al., XCOM: Photon Cross Section Database (version 1.3), National Institute of Standards and Technology, Gaithersburg MD (2005).

22. M. O. Krause, J. Phys. Chem. Ref. Data (USA) **8**, 307 (1979).

23. J. H. Scofield, At. Data Nucl. Data Tab. **14**, 121 (1974).

24. G. Apaydin, V. Aylikci, E. Cengiz et al., Radiat. Phys. Chem. **77**, 923 (2008).

25. A. S. Bennal and N. M. Badiger, Nucl. Instr. Meth. B **247**, 161 (2006).

26. R. Durak and Y. Ozdemir, J. Phys. B **31**, 3575 (1998).

27. M. Ertuğral, O. Dogan, O. Şimsek et al., Phys. Rev. A **55**, 303 (1997).

28. G. C. Nelson and B. G. Saunders, Phys. Rev. **188**, 108 (1969).

29. B. Ertuğral, G. Apaydin, U. Cevik et al., Radiat. Phys. Chem. **76**, 15 (2007).

30. J. H. McCrary, L. V. Singman, L. H. Ziegler et al., Phys. Rev. A **4**, 1745 (1971).

31. A. G. de Pinho, Phys. Rev. A **3**, 905 (1971).

32. B. Ertuğral, G. Apaydin, H. Baltas et al., Spectrochimica Acta B **60**, 519 (2005).

33. A. S. Bennal, K. M. Niranjan, and N. M. Badiger, J. Quant. Spectrosc. Radiat. Transfer **111**, 1363 (2010).

34. M. R. Khan and M. Karimi,X-ray Spectrom. **9**, 32 (1980).